NACA RM L56A25

NACA

RESEARCH MEMORANDUM

TWO EXPERIMENTS ON APPLICATIONS OF THE TRANSONIC AREA RULE TO ASYMMETRIC CONFIGURATIONS

By James Rudyard Hall

Langley Aeronautical Laboratory
Langley Field, Va.

NATIONAL ADVISORY COMMITTEE
FOR AERONAUTICS

WASHINGTON

April 20, 1956
Declassified May 29, 1959

NATIONAL ADVISORY COMMITTEE FOR AERONAUTICS

RESEARCH MEMORANDUM

TWO EXPERIMENTS ON APPLICATIONS OF THE TRANSONIC AREA RULE TO ASYMMETRIC CONFIGURATIONS

By James Rudyard Hall

SUMMARY

Two experiments concerning the transonic area rule have shown that the wing of a configuration has a powerful effect as a dividing plate.

The approximation of store plus interference wave drag (near a Mach number of 1) for underwing stores was more accurately made by considering the normal area development of the configuration above and below the wing separately instead of the total area development.

Indenting a fuselage on only one side of the wing to allow for the exposed wing volume gave appreciably less pressure-drag reduction than that obtained with a symmetrically indented fuselage. A small reduction of pressure drag was effected over the unindented configuration near a Mach number of 1.

INTRODUCTION

The transonic area rule promulgated in reference 1 has been shown to be useful as a means of assessing the zero-lift drag characteristics of many configurations. Basically, the transonic area rule states that the pressure field around a configuration near the speed of sound is duplicated by the field around the equivalent body of revolution of that configuration. From this concept two applications have developed, namely: (1) the approximation of the pressure drag of a configuration by measuring the pressure drag of its equivalent body of revolution and (2) the reduction of configuration pressure drag by modifications designed to provide a more favorable axial distribution of the cross-sectional area. The question has arisen as to the extent to which the above applications are affected by asymmetry. For example, external stores carried below an aircraft wing may be somewhat confined in their effect because the wing can act as a dividing plate confining the disturbance due to the nacelles to one side of the wing. In such a case the axial area development of

the nacelles is not equivalent to an annulus completely around the body. Also, reduction of wing pressure drag by indenting the fuselage entirely above the wing would not be expected to be as effective as symmetrical indentation. These are important practical considerations because most aircraft configurations cannot be symmetrical because of design and operational requirements. Although many investigations (refs. 1 to 4, for example) have shown that the area rule can be applied successfully to the approximation and reduction of pressure drag of aircraft configurations, little work has been reported on quantitative measurements of the effects of asymmetry, and in particular on the effect of the wing as a dividing plate. The present report presents the results of two brief investigations on this subject conducted by the Pilotless Aircraft Research Division of the Langley Aeronautical Laboratory. The experiments concern the extent to which a wing acts as a dividing plate with regard to: (1) the representation on an equivalent body of nacelles mounted below the wing and (2) the effect of locating fuselage indentation (for a wing) on only one side of the wing.

The experiments were performed at the Langley Pilotless Aircraft Research Station at Wallops Island, Va., utilizing the 6-inch helium gun, and covered a Reynolds number range based on model length from 9×10^6 at a Mach number of 1.35 to 5×10^6 at a Mach number of 0.8.

SYMBOLS

a	acceleration, ft/sec^2
A	cross-sectional area, $in.^2$
C_D	$\frac{Drag}{qS}$
ΔC_D	pressure drag coefficient, supersonic drag coefficient minus subsonic drag coefficient
g	acceleration of gravity, 32.2 ft/sec^2
l	fuselage length, in.
M	Mach number
q	dynamic pressure, lb/ft^2
r	radius of equivalent body, in.

S total wing area of the configuration upon which the models were based scaled to the size of the models, ft^2

W weight, lb

x fuselage station, in.

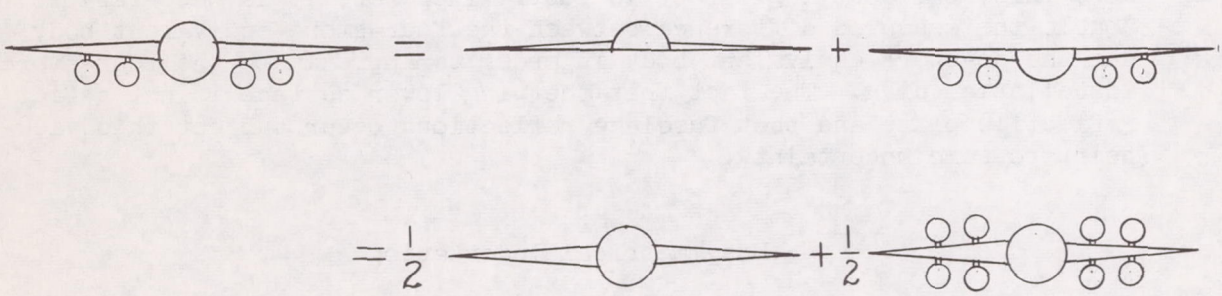
γ flight-path angle, deg

CONCEPT

This section discusses applications of the transonic area rule for estimating the transonic drag rise of aircraft configurations with stores mounted below the wing and of the transonic installation drag due to the stores. The underlying principle of the technique presented is based on the assumption that the wing acts as a dividing plate and that a configuration may be represented by two equivalent bodies of revolution as determined by the geometry above and below the wing plane of symmetry. Of course, the usual restriction of "near Mach number unity" applies to these applications of the area rule.

Underwing Stores

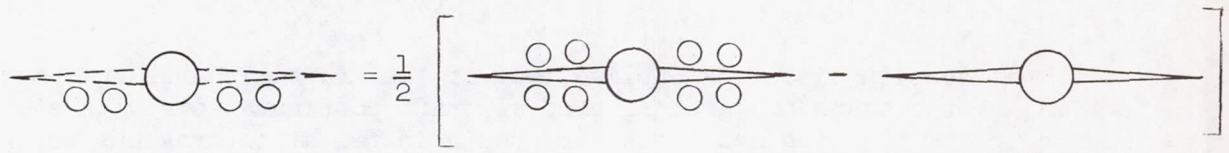
A configuration with stores mounted below the wing may be considered to be divided along the wing plane of symmetry into two parts, one with stores and one without stores, as is depicted in sketch A.



Sketch A

Then the pressure drag of the original configuration may be thought of as half the sum of the pressure drag of a storeless configuration and a symmetrical eight-store configuration. Inasmuch as the latter two are symmetrical, their equivalent bodies of revolution may be used to approximate their pressure drag. Hence, by averaging the pressure drag of the two equivalent bodies of revolution it should be possible to obtain the pressure drag of a configuration having stores mounted below the wing.

Sketch B illustrates how the above principle may be used to approximate the installation drag of underwing stores.



Store in presence of body | Eight-store equivalent body | No-store equivalent body

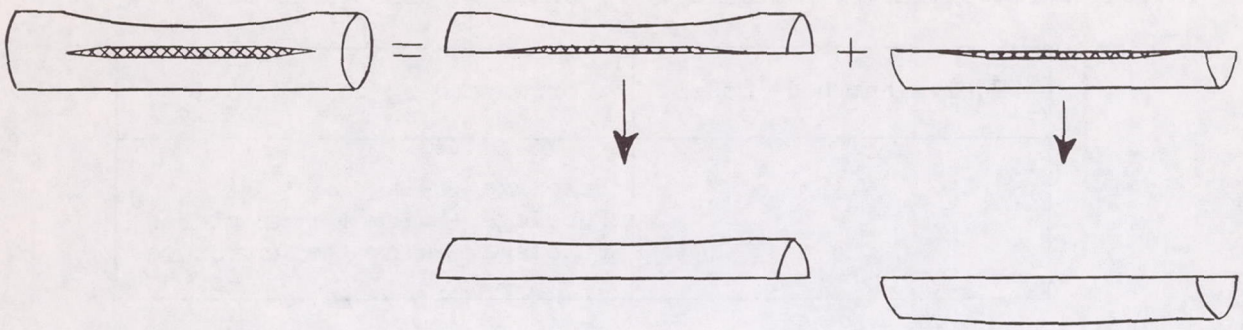
Sketch B

Since the eight-store and no-store configurations are symmetrical their equivalent bodies can be employed to obtain the eight-store and no-store configuration pressure drag. Half the difference of the two should approximate the pressure drag plus interference of four stores.

Installation drag of underwing stores may also be estimated in a different manner using the area rule concept. At a Mach number of 1 the four stores of the configuration are reflected by the wing giving an apparent doubling of store pressure drag. When the four-store configuration is converted to an equivalent body on the basis of the transonic area rule, the doubling effect is lost. Therefore it is necessary to double the measured difference between the four-store equivalent body and the no-store equivalent body in order to approximate the four-store installation drag. The fact that the wing lower surface is not a flat reflection plane and that fuselage reflections occur subject this viewpoint to some uncertainty.

Unsymmetrical Indentation

A wing-body combination indented entirely above the wing to compensate for the exposed wing cross-sectional-area distribution can be represented as shown in sketch C, wherein the configuration is divided into two parts along the wing plane of symmetry.



Sketch C

The upper half contains an indentation for the entire wing cross-sectional area, whereas the lower half is unindented. If the wing cross-sectional area of each half were distributed along its fuselage, the indentation of the upper half would be reduced in severity to a normal transonic indentation while the unindented half would acquire a normal transonic bump. (Comparatively, if a symmetrically indented configuration were split as above and converted to two equivalent half-bodies, the wing cross-sectional area would exactly compensate the indentations, giving two smooth, unindented equivalent half-bodies. Also, if an unindented configuration were split and converted to two equivalent half-bodies, each would have a normal transonic bump.) These considerations show that the only advantage to be expected from such an asymmetrically indented configuration over an unindented configuration arises from a small reduction of pressure drag due to replacement of a wing bump on one side of the fuselage by an equivalent wing indentation. Inasmuch as the wing is not completely effective as a dividing plate, the indentation above the wing should alleviate the pressure drag due to the lower half of the configuration, and the pressure drag of the asymmetrically indented configuration should be somewhat lower than predicted assuming isolation of the upper and lower halves of the configuration.

CONFIGURATIONS

The two aspects of the effects of asymmetry on applications of the area rule which are reported herein will be denoted as part I and part II of the investigation. The two aspects employed different configurations.

Part I of the investigation utilized bodies of revolution of the configuration shown in figure 1. These were denoted as follows:

Equivalent body model	Corresponding configuration
1	Fuselage + wing
2	Fuselage + wing + four stores
3	Fuselage + wing + eight stores

The nondimensional area distribution of the basic configuration (and hence of the models) is shown in figure 2. A drawing of models 1 to 3 and their coordinates is given in figure 3. Photographs of the models are given in figure 4. The word "fuselage" as used in the table above for the equivalent body models is the fuselage of the original configuration including the cross-sectional area of the tails, with the cross-sectional area of the stabilizing fins used on the models subtracted. Both fin areas were similar so that the exchange of volume was small.

Part II of the program concerned the evaluation of the merits of indenting the fuselage to compensate for the complete cross-sectional area of a delta wing above the wing only, compared to symmetrical indentation. A delta wing was used because it was felt that it would more effectively isolate the upper and lower halves of the fuselage in the region of the wing than a swept wing of equivalent aspect ratio, and hence provided a more severe test. The configurations employed are tabulated below and depicted in figure 5.

Model	Description
4	Wingless
5	Winged, unindented
6	Winged, symmetrically indented
7	Winged, indented above wing only

The delta wing which employed a simple hexagonal section was 3.6 percent thick at the mean aerodynamic chord and had a leading-edge sweep angle of $52\frac{1}{2}^{\circ}$. The ratio of wing cross-sectional area to fuselage area was chosen to be as large as possible without producing excessively high slopes on the fuselage indentations. The high-fineness-ratio nose was used to give low pressure drag in order that the effect of indentation would be a larger percentage of the total drag. The cylindrical fuselage section forward of the wing was intended to establish parallel

flow somewhat before the indented region. The cylindrical section behind the wing and the rather low boattail angle were used to reduce the flow angles over the afterbody and minimize the base drag. The nondimensional area distribution and radius distribution of the models is given on figure 6. Photographs of typical models are given in figure 7.

The models were machined of aluminum alloy and brass. The brass noses were ballasted to give a static margin of 2 to 3 body diameters.

TESTS

The models were tested by firing them from the 6-inch helium gun at the Langley Pilotless Aircraft Research Station, Wallops Island, Va. In operation a model is placed in a 6-inch-diameter balsa sabot in the breech of the gun. A push plate behind the sabot bears against it and the model. A quick-opening valve admits helium to the gun barrel under about 200 lb/sq in. pressure accelerating the sabot assembly down the 23-ft barrel to supersonic velocities. Upon emerging from the barrel the three segments and the push plate peel away, falling to earth within 50 yards. The model continues to decelerate along a ballistic trajectory during which period a continuous velocity history is obtained by means of a CW Doppler velocimeter. Atmospheric conditions aloft were obtained by radiosonde measurements from an ascending balloon released at the time of the experiment. A flight path was obtained by integrating the velocity along a ballistic trajectory. The model deceleration was compiled from the velocity history corrected for effects of wind and the coefficient of drag was compiled from the relationship

$$C_D = -\frac{W}{gqS}(a + g \sin \gamma)$$

The maximum systematic errors in the drag coefficient and Mach number measurements are estimated to be ± 0.0010 and ± 0.008, respectively.

The Reynolds number of the tests, based on a model length, varied from 9×10^6 at a Mach number of 1.35 to 5×10^6 at a Mach number of 0.8.

RESULTS AND DISCUSSION

The measured drag coefficients of the part I equivalent body models (external store investigation) and of the configuration models (ref. 5) from which the equivalent body models were derived are shown in figure 8. In figure 9 are shown the corresponding pressure drag coefficients, which are assumed to be given by the drag rise above the subsonic level. The

pressure drag coefficients of the equivalent body models 1 and 2 are substantially lower than those of the corresponding configurations. This discrepancy has been noted in several other similar comparisons for swept-wing configurations (refs. 1, 2, and 4). The hypothesis discussed in the section entitled "Concept," in which the pressure drag of an asymmetric configuration having four stores mounted beneath the wing was said to equal the averaged pressure drag of the no-store and eight-store equivalent bodies, is shown in figure 10 to improve the agreement obtained without using this concept. Inasmuch as a swept-wing configuration was employed, the equivalent body pressure drag would be expected to be lower than configuration drag, as is the case. Although this single experiment is not conclusive, it appears possible that this concept might be found useful in the application of the area rule to the approximation of pressure drag of configurations with stores mounted below the wing, especially for delta and straight wings for which equivalent body pressure-drag approximations are more correctly made.

The store pressure drag coefficients derived from the equivalent body tests are compared in figure 11 with the isolated store pressure drag and the installation drag from reference 5.

It can be seen that interference drag is about ten times the magnitude of the isolated stores pressure drag. The method of predicting store drag by taking half the difference between the eight-store equivalent body and the no-store equivalent body gives reasonably accurate results near a Mach number of 1. In particular, it indicates the early drag-rise Mach number and the high level of interference drag for the installation. The approximate method which involves taking twice the difference between the four-store equivalent body and the no-store equivalent body gives poorer agreement with the measured drag-rise Mach number and level of installation drag. As a matter of interest the store drag obtained by taking the difference between the four-store equivalent body and the no-store equivalent body is given and is seen to give poorer agreement in the transonic region. The improved agreement above the transonic region must be considered fortuitous since the reflection effects previously discussed apply only very close to a Mach number of 1. It appears from these comparisons that a more accurate prediction of store-plus-interference wave drag near a Mach number of 1.0 can be made by considering the area development of the configuration above and below the wing plane separately, instead of the total cross-section area of the wing-body-stores combination.

The total-drag and pressure drag coefficients for the part II models are shown in figure 12. The results show that the symmetric indentation yielded substantial drag reductions near a Mach number of 1.0. These reductions became smaller with increasing Mach number. The asymmetric indentation was much less effective near a Mach number of 1.0 and at high Mach numbers actually increased the pressure drag over the unindented configurations. These results are in agreement near a Mach number of 1

with the previously discussed concept, in that they show further evidence that the wing acts as a dividing plane.

CONCLUSIONS

1. Two experiments concerning the transonic area rule have shown that the wing of a configuration can exert a powerful effect as a dividing plate.

2. The approximation of store plus interference wave drag (near a Mach number of 1) for underwing stores was more accurately made by considering the normal area development of the configuration above and below the wing separately instead of the total area development.

3. Indenting a fuselage on only one side of the wing to allow for the exposed wing volume gave appreciably less pressure-drag reduction than was obtained with a symmetrically indented fuselage. A small reduction of pressure drag was effected over the unindented configuration near a Mach number of 1.

Langley Aeronautical Laboratory,
National Advisory Committee for Aeronautics,
Langley Field, Va., January 10, 1956.

REFERENCES

1. Whitcomb, Richard T.: A Study of the Zero-Lift Drag-Rise Characteristics of Wing-Body Combinations Near the Speed of Sound. NACA RM L52H08, 1952.

2. Hall, James Rudyard: Comparison of Free-Flight Measurements of the Zero-Lift Drag Rise of Six Airplane Configurations and Their Equivalent Bodies of Revolution at Transonic Speeds. NACA RM L53J21a, 1954.

3. Whitcomb, Richart T.: Recent Results Pertaining to the Application of the "Area Rule." NACA RM L53I15a, 1953.

4. Hoffman, Sherwood: An Investigation of the Transonic Area Rule by Flight Tests of a Sweptback Wing on a Cylindrical Body With and Without Body Indentation Between Mach Numbers 0.9 and 1.8. NACA RM L53J20a, 1953.

5. Henning, Allen B.: The Effects of Wing-Mounted External Stores on the Trim, Buffet, and Drag Characteristics of a Rocket-Propelled Model Having a 45° Sweptback Wing. NACA RM L54B19, 1954.

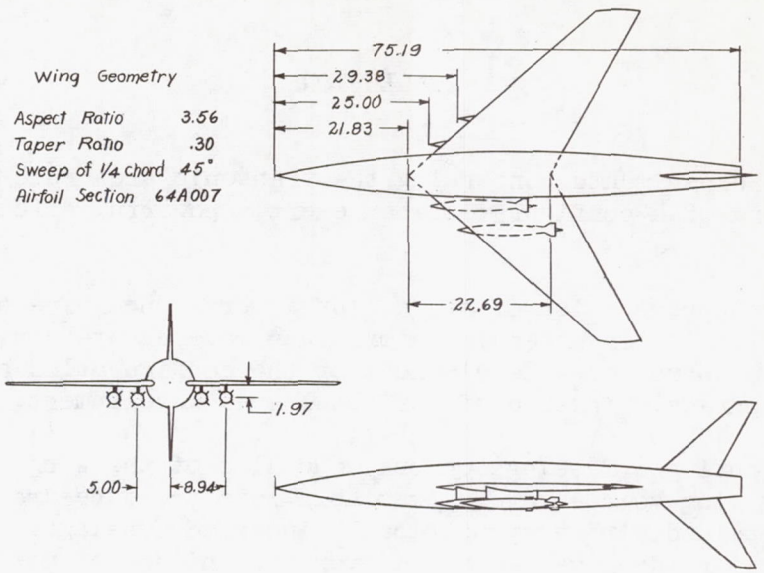


Figure 1.- Configuration utilized as a basis for equivalent body tests in part I of the current investigation. All dimensions are in inches.

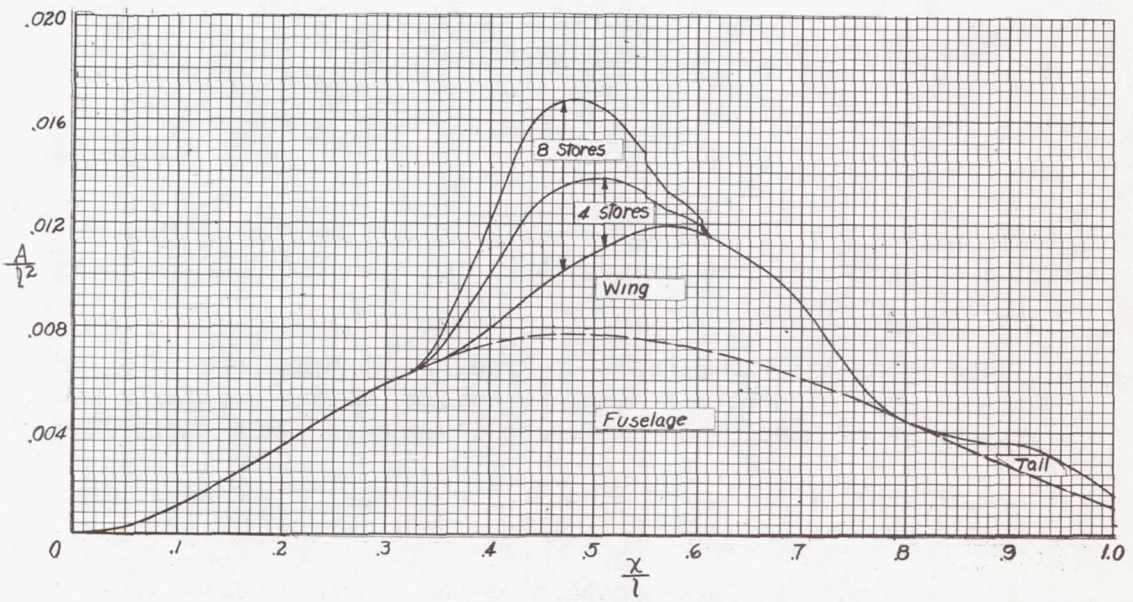
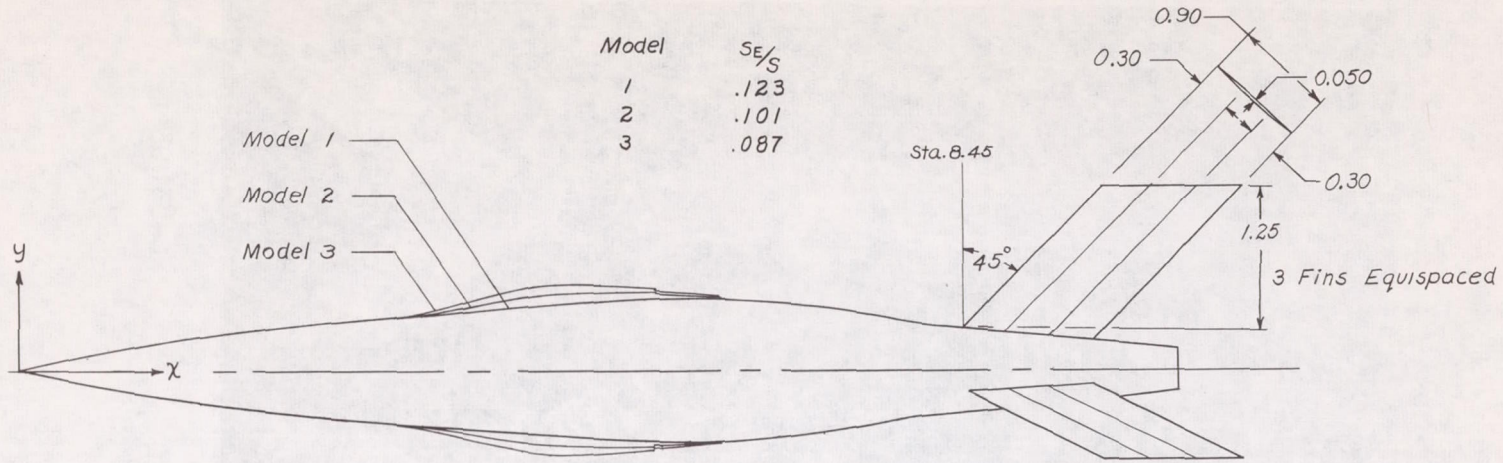


Figure 2.- Nondimensional area distribution of basic configuration.

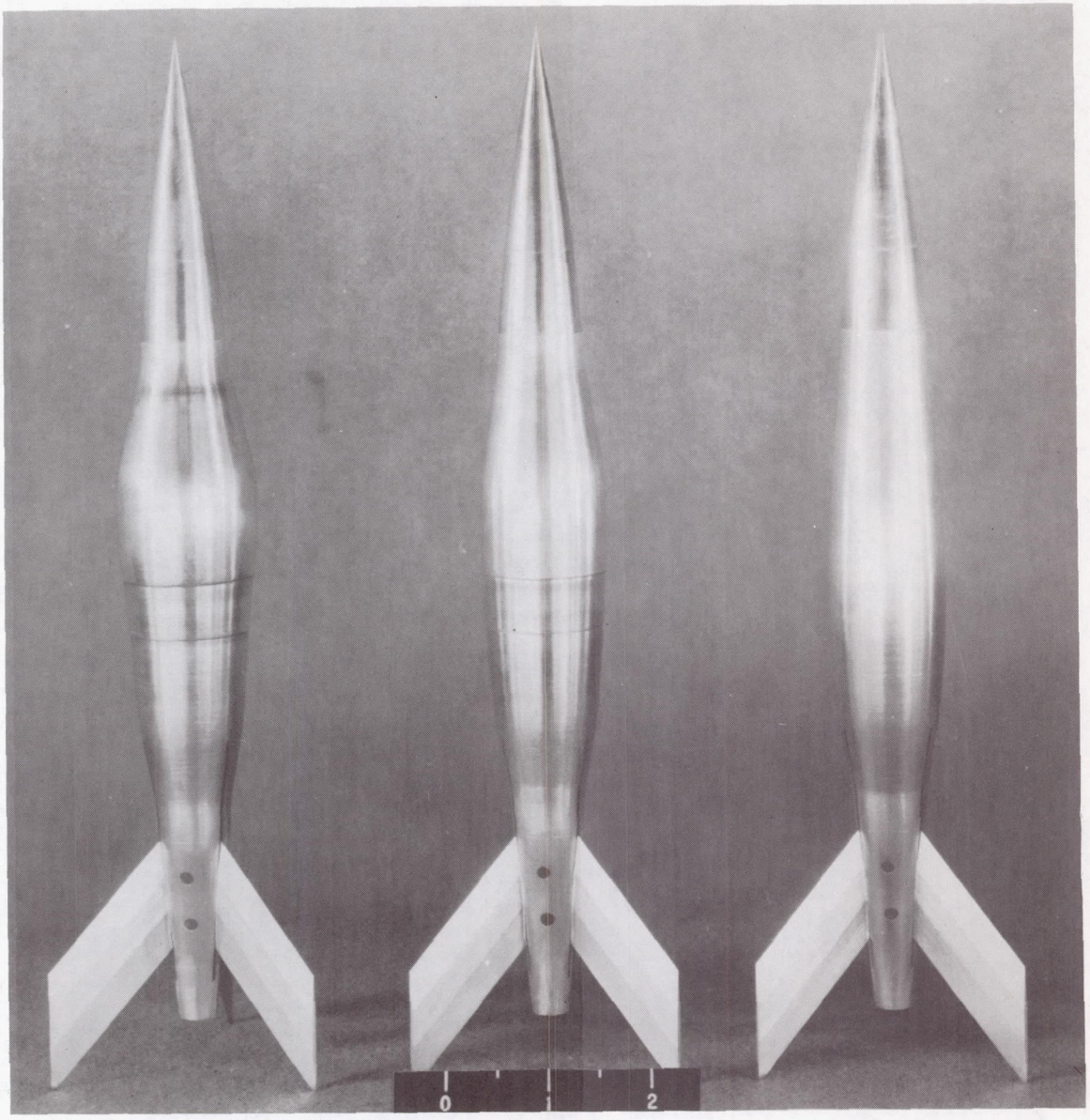


x	y Model 1	2	3
0			
.2	.042	→	→
.4	.082		
.6	.120		
.8	.156		
1.0	.190		
.2	.221		
.4	.252		
.6	.282		
.8	.310		
2.0	.335		
.2	.360		
.4	.382		
.6	.402		
.8	.422		
3.0	.439		
.2	.454		
.37	.464	→	→
.6	.478	.490	.500
.8	.493	.528	.559
4.0	.510	.559	.602

x	y Model 1	2	3
4.2	.529	.595	.653
.4	.547	.630	.700
.6	.566	.658	.740
.8	.583	.676	.757
5.0	.599	.684	.760
.2	.612	.687	.755
.36	—	.684	.744
.40	.623	—	—
.50	—	.681	.732
.6	.612	.678	.722
.7	—	.673	.708
.7	—	.670	.703
.8	.637	.664	.690
.9	—	.658	.676
6.0	.639	.655	.670
.1	—	.649	.661
.2	.634	.643	.652
.27	—	.638	.645
.27	—	.635	.640
.40	.626	.627	.629
6.50	.622	—	—

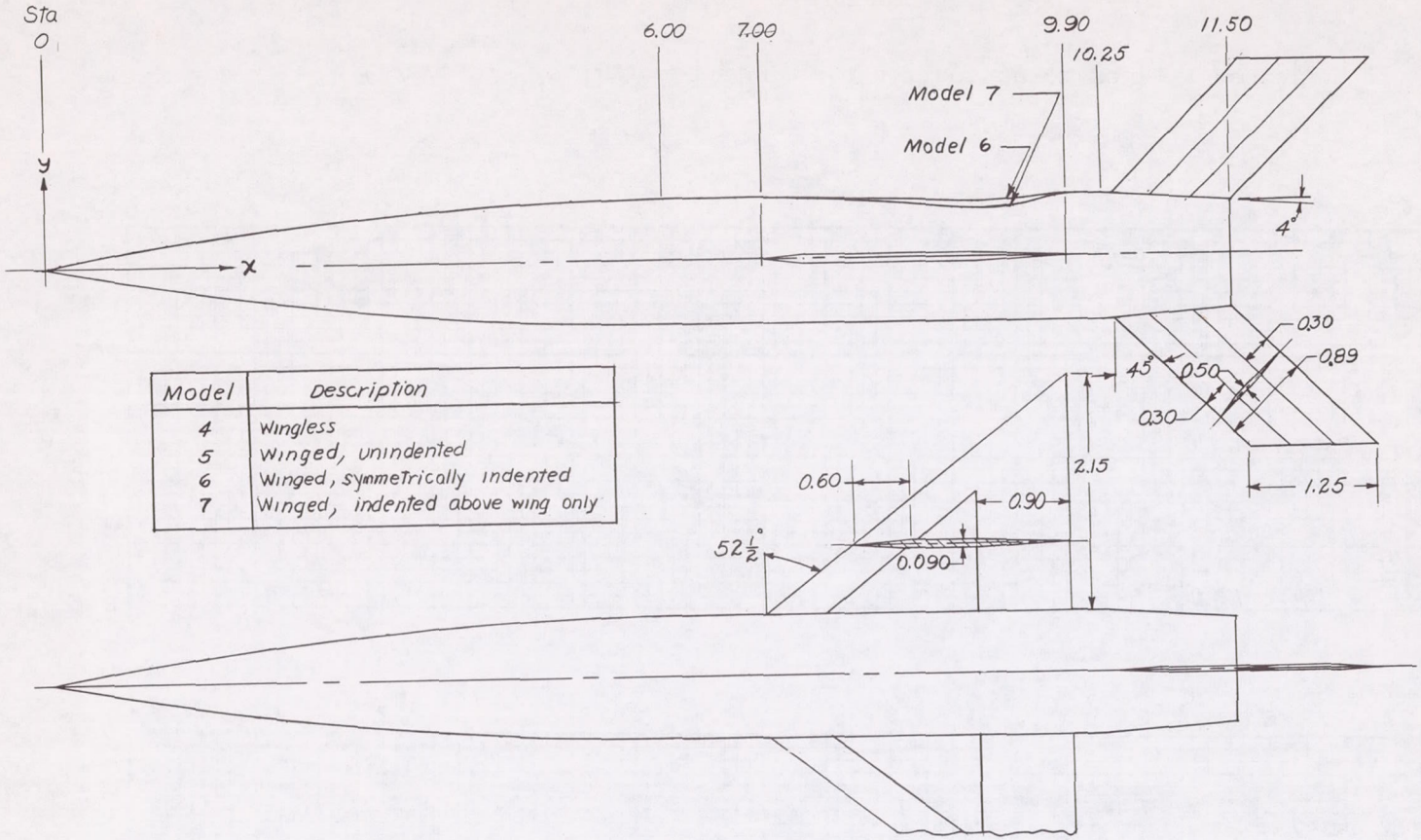
x	y Model 1	2	3
6.6	.613	→	→
.8	.598		
7.0	.581		
.2	.560		
.4	.532		
.6	.494		
.8	.456		
8.0	.421		
.1	.408		
.2	.400		
.4	.386		
.6	.369		
.8	.348		
9.0	.325		
.2	.307		
.4	.292		
.6	.274		
.8	.256		
10.0	.237		
.2	.217		
10.371	.194	→	→

Figure 3.- Coordinates of models 1 to 3. All dimensions are in inches.



L-83803

Figure 4.- Photograph of models 3, 2, and 1.



Model	Description
4	Wingless
5	Winged, unindented
6	Winged, symmetrically indented
7	Winged, indented above wing only

x	y	
	Model 6	Model 7
0	0	
.4	.077	→
.8	.150	
1.2	.216	
1.6	.277	
2.0	.333	
2.4	.384	
2.8	.429	
3.2	.470	
3.6	.504	
4.0	.534	
4.4	.558	
4.8	.576	
5.2	.589	
5.6	.597	
6.0	.600	
7.0	.600	→
7.2	.599	.597
7.4	.595	.589
7.6	.588	.575
7.8	.581	.561
8.0	.573	.545
8.2	.566	.529
8.4	.588	.512
8.6	.550	.494
8.8	.542	.476
9.0	.534	.458
9.2	.540	.473
9.4	.552	.498
9.6	.568	.535
9.9	.600	.600
10.25	.600	.600
	4° Taper	
11.5	.523	.523

Figure 5.- Configurations employed in part II of investigation.

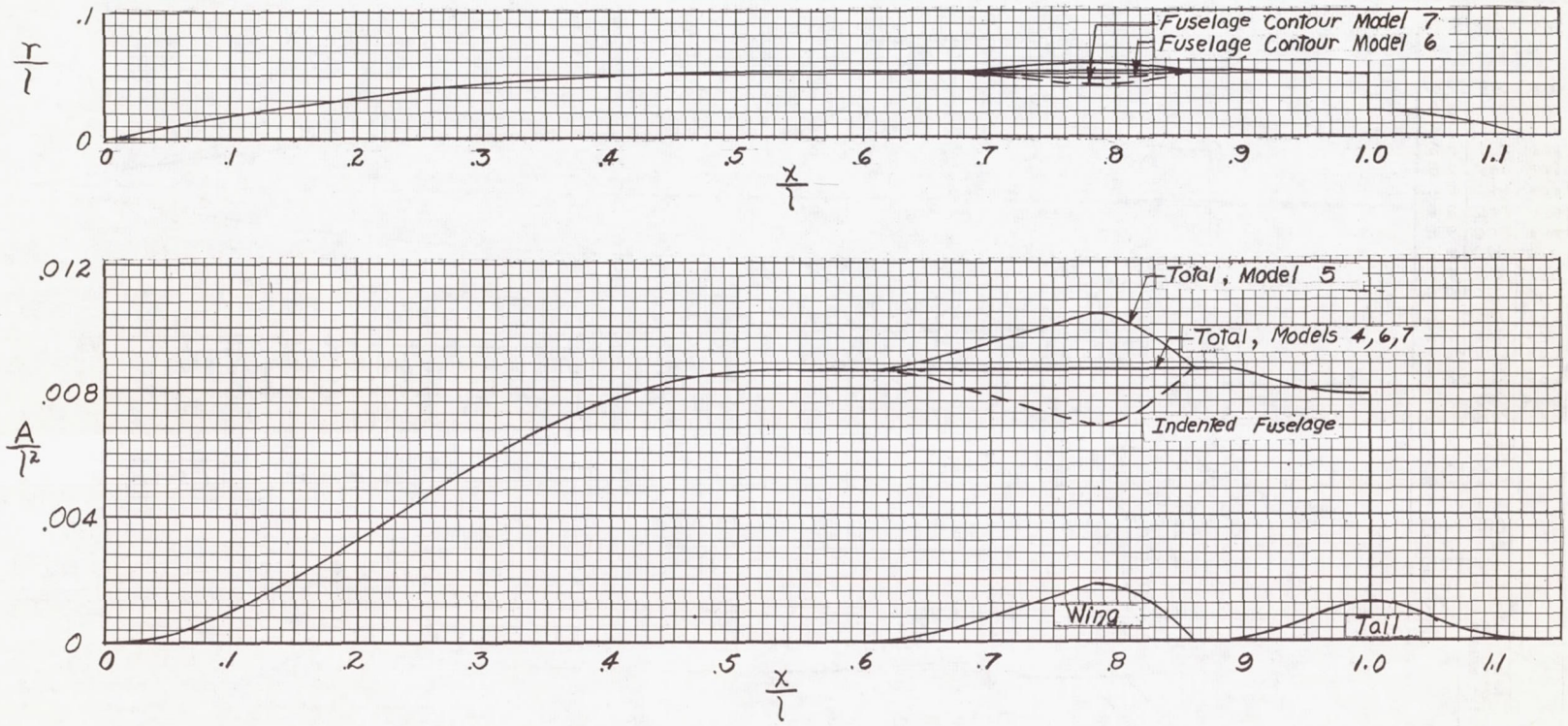
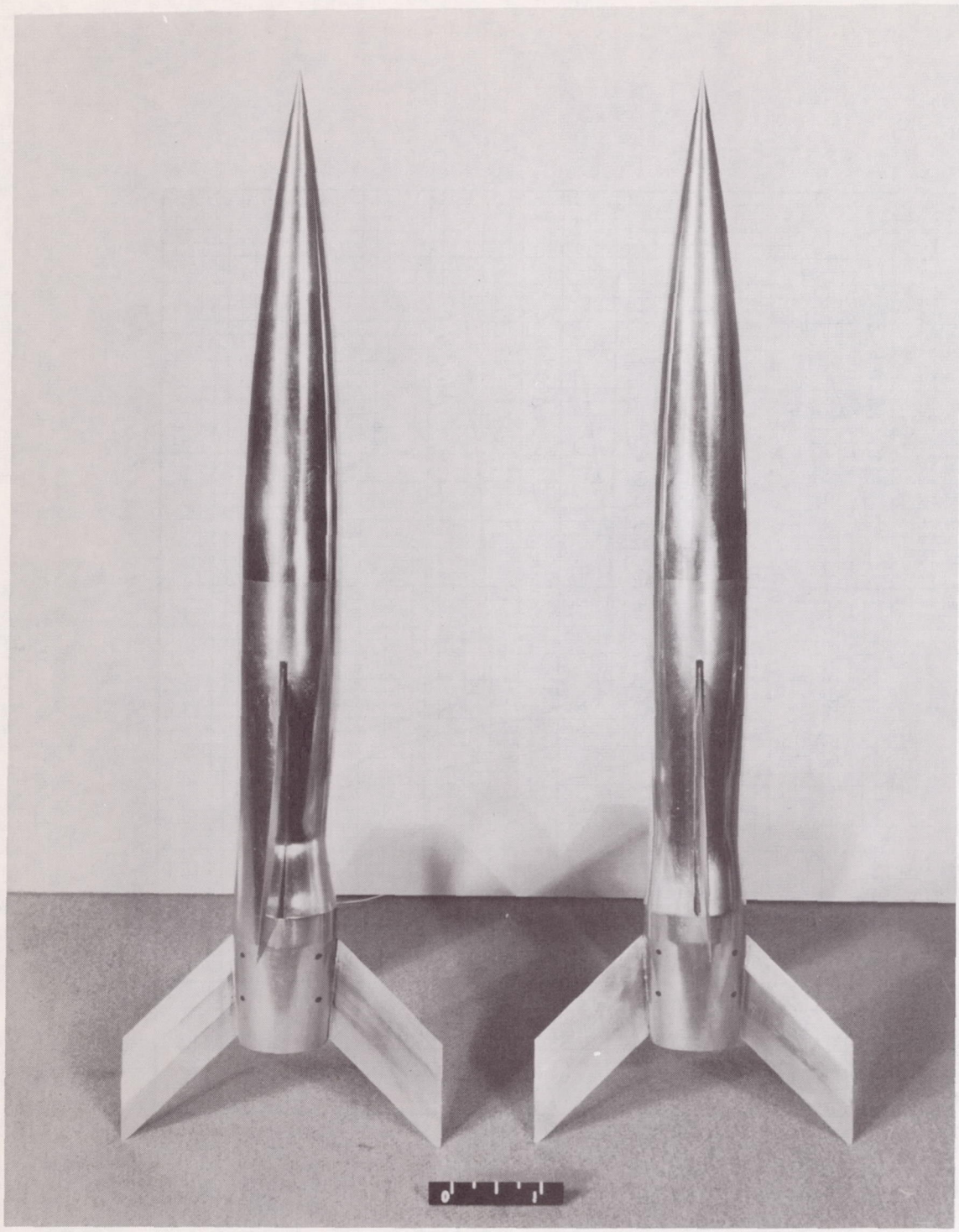


Figure 6.- Nondimensional area distribution of part II models.



L-80531

Figure 7.- Photograph of models 6 and 7 showing fuselage indentations and typical construction details.

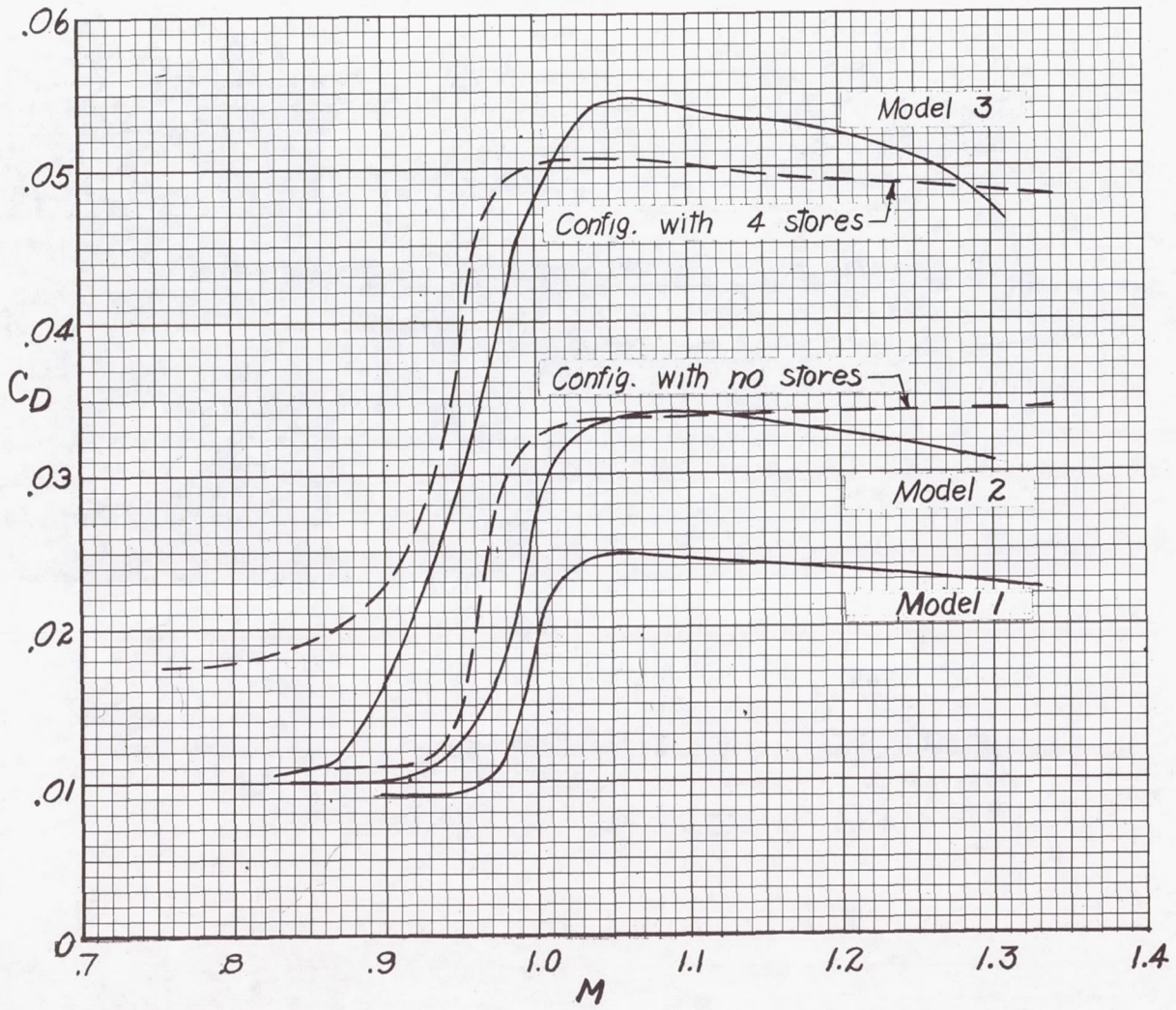


Figure 8.- Drag coefficients measured for the part I models and the configurations upon which they were based.

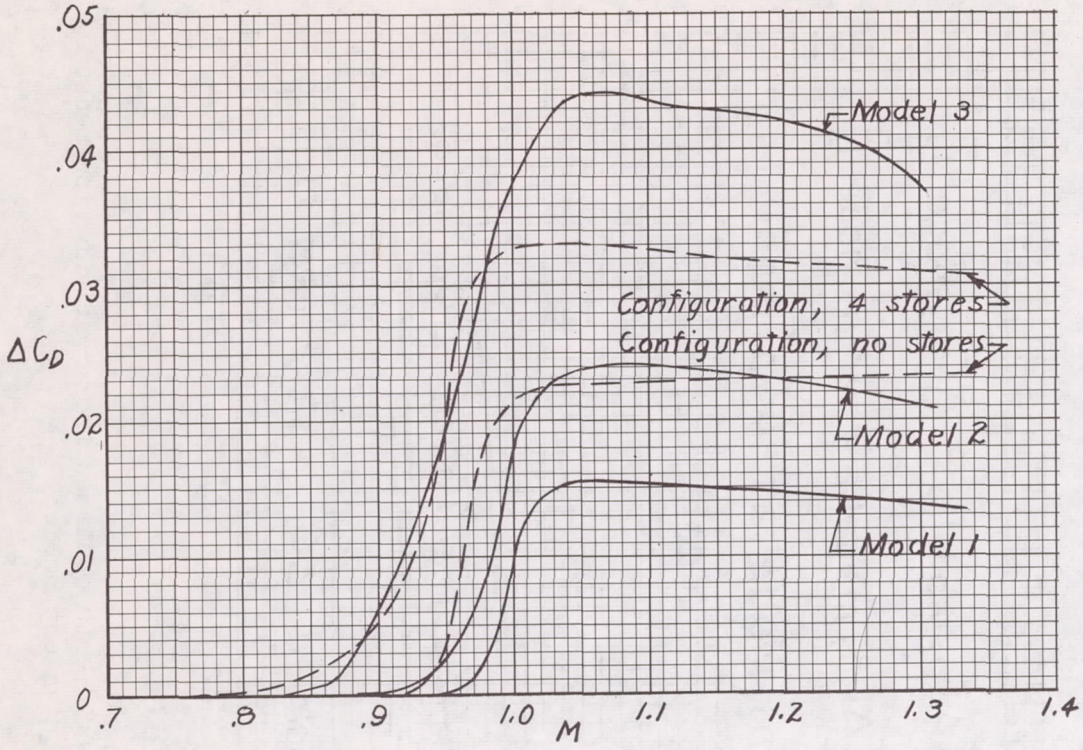


Figure 9.- Pressure drag coefficients.

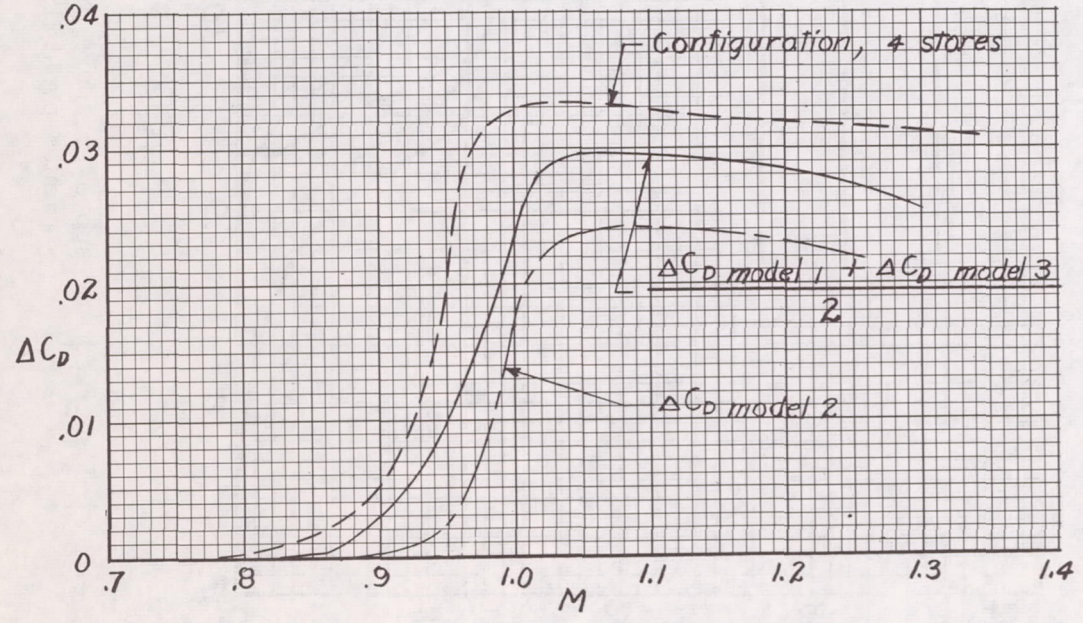


Figure 10.- Comparison of pressure drag coefficients of four-store configuration with those derived from equivalent body tests.

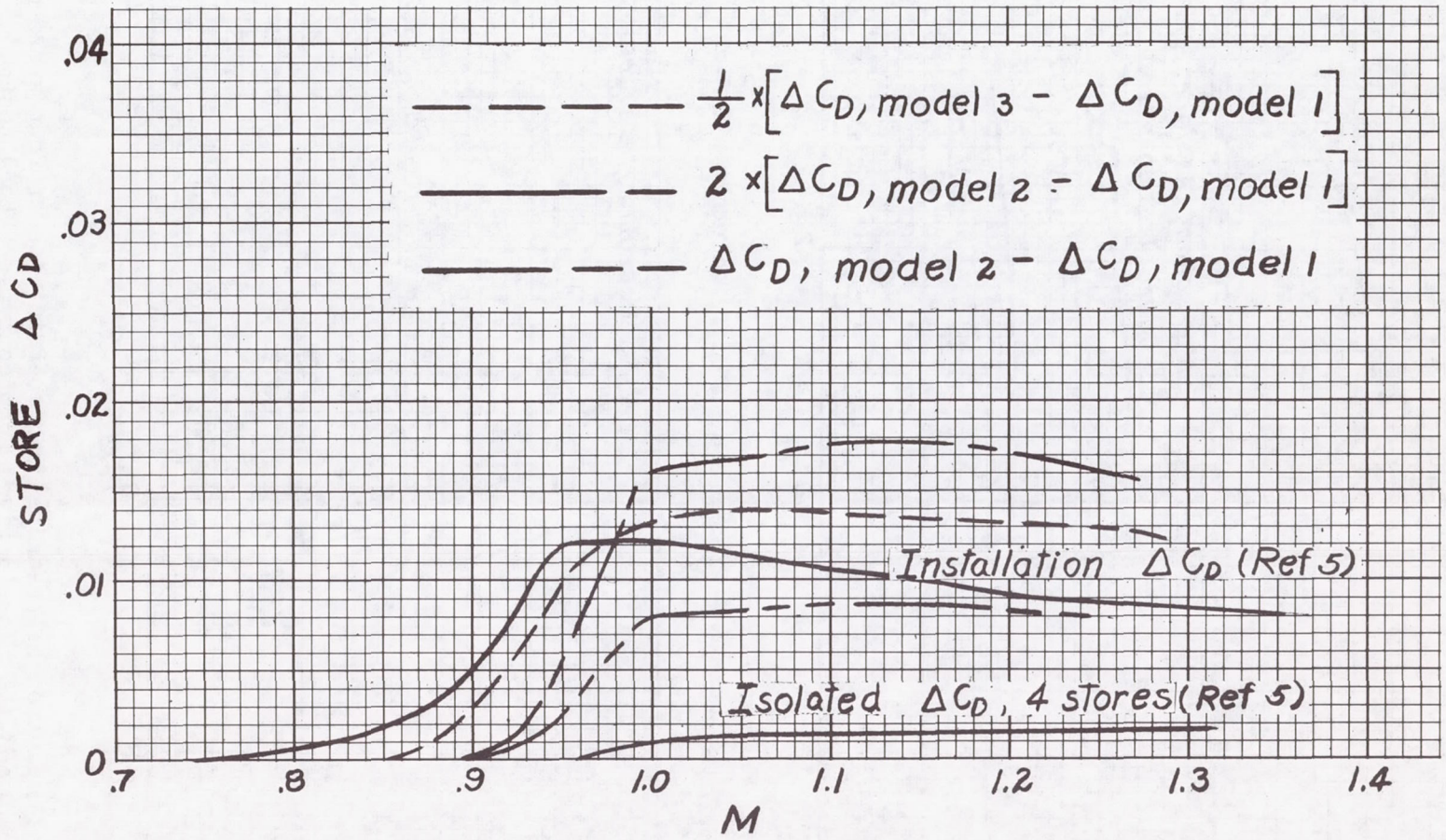
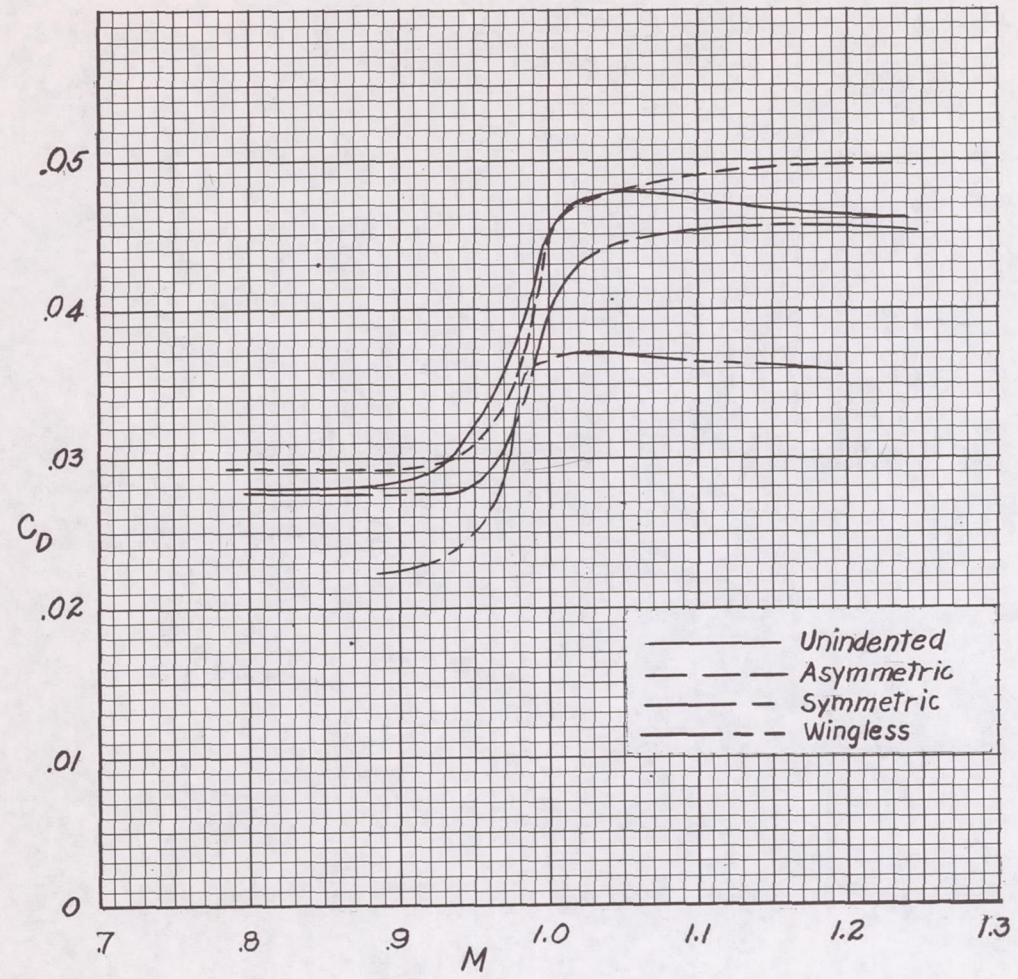


Figure 11.- Comparison of store pressure drag coefficients obtained from configuration measurements by utilizing equivalent bodies.



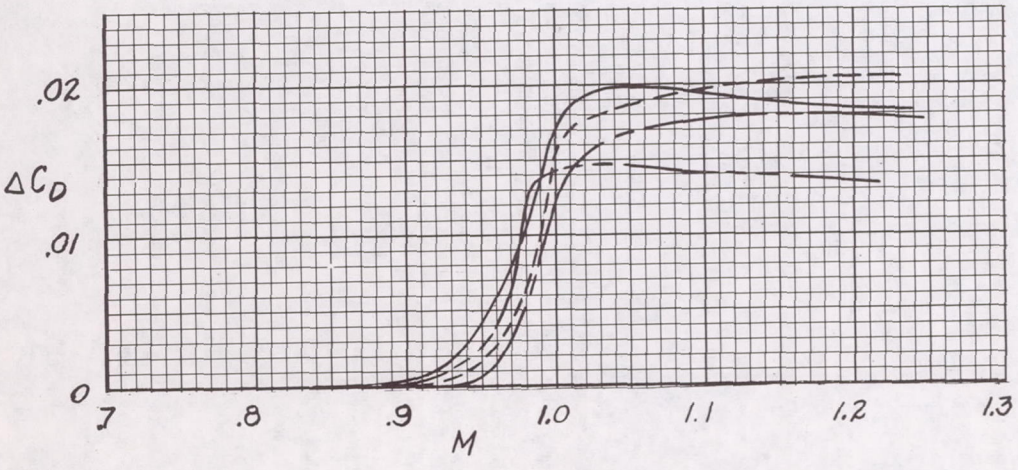


Figure 12.- Drag coefficient and pressure drag coefficient for part II mod